
My Data Literacy Project

(Replace this with your Project Title)

Zhi Jing * Enrico Vesentini * Tài Thái * Jonas Thumbs * Baisu Zhou *

Abstract

While colorimetry devices can accurately measure colors of objects, they are too expensive for daily usage such as detecting color of a scratched surface for repainting. Color picking from images captured by a smartphone is subject to distortion due to ambient light. We statistically analyze a deterministic and a data-driven color correction method which improves the accuracy of color detection using smartphone images, showing that simple, post-hoc correction can greatly improve the quality of color measurements done by smartphones.

1. Introduction

Measuring color accurately is a common problem in daily life, e.g., when a surface needs to be repainted in the same color. Devices that can carry out this task, the so-called *colorimeters*, are available commercially and usually cost several hundred dollars. There are smartphone apps that claim to offer the same service for free by using the built-in camera. A challenge in this approach is how to deal with the effect of ambient light. Simply picking the color from a photo is not ideal because hue, saturation, and brightness depend heavily on the lighting conditions. One way to address this issue is to capture the color of a white reference object (e.g., a white piece of paper) at the same time and use this to correct for the ambient light.

In this study, we want to find a sufficiently accurate approach to correct for ambient light and analyze the usability of measurements from such an app for color detection. While smartphone cameras store colors in RGB format, the RGB color space is not suitable for our analysis, because the distance between two points in the RGB space does not align with the perceived difference between two colors. In our

*Equal contribution . Correspondence to: BZ <baisu.zhou@student.uni-tuebingen.de>.

Project report for the “Data Literacy” course at the University of Tübingen, Winter 2025/26 (Module ML4201). Style template based on the [ICML style files 2025](#). Copyright 2025 by the author(s).

analysis, we use the CIELAB (or $L^*a^*b^*$) color space, designed by Commission Internationale de l’Éclairage (CIE)¹ for colorimetric applications. Every color in the RGB space can be mapped non-linearly to a point (L^*, a^*, b^*) in the $L^*a^*b^*$ space, where the L^* coordinate represents lightness and the a^*, b^* coordinates control the hue. The Euclidean distance on the $L^*a^*b^*$ space reflects the perceived difference between colors.

To evaluate the performance of the correction methods, we define an accuracy thresholds. The first corresponds to the human chromatic sensitivity threshold, while the second represents a small but perceptible color difference. The smallest wavelength difference that can be perceived as a chromatic difference under constant luminance conditions (“just noticeable difference”) is approximately 1 nm, which corresponds to about an Euclidean distance of approximately 1.27 in the $L^*a^*b^*$ color space (Oleari, 2015). The authors further mentioned that a few multiples of the just noticeable difference can still be considered small. Accordingly, we define the Euclidean error 6 (approximately five times the just noticeable difference) as the *small color difference threshold* in our study.

We have developed our own color measurement app with built-in correction using white reference. As the transformation from RGB to $L^*a^*b^*$ is intended for measurements under CIE’s D65 lighting condition (Oleari, 2015), we collected data using our app under a lighting condition similar to D65 (Section 2.1). We further compared the app’s correction-by-scaling method (??) with a modeling approach (Section 2.3). While the model provides insights into the color correction mechanism, the scaling method proves to be more robust (Section 3).

2. Data and Methods

2.1. Data Collection

We used a color reference sheet designed for camera calibration as the object from which we collect data. The reference sheet consists of 24 color cards and provides ac-

¹In Enligh: International Commission on Illumination. Website: <https://cie.co.at/>.

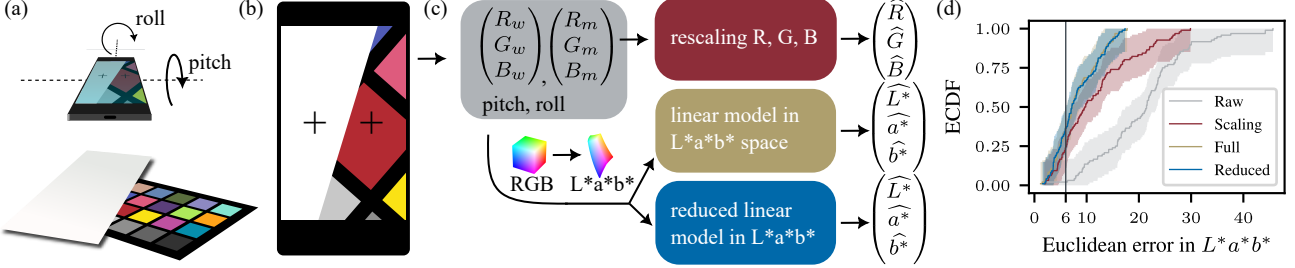


Figure 1. Workflow of data collection and color correction. (a) Color measurements taken by smartphone with white paper reference. (b) Illustration of our color detection app. During data collection, we covered all color cards but the one under measurement rather than exposing them as in the illustrative figure. (c) Color correction methods. (d) ECDFs of Euclidean distances from the raw and corrected colors to the ground truths. The shaded areas are 95% Dvoretzky–Kiefer–Wolfowitz confidence bands (Dvoretzky et al., 1956; Wasserman, 2004). The dashed vertical line indicates the small color difference threshold.

curate ground-truth RGB values for each color. We used two phones, Google Pixel 8 Pro and Samsung Galaxy S21 Ultra, for data collection. The data were collected indoors on a desk in front of the window under natural daylight on November 19, 2025 in Tübingen, Germany. The procedure is as follows.

We placed a white piece of paper (called *white reference* in the following) with a cut-out square hole over the array of colors to ensure similar conditions for all measurements. Only one color card was visible to the camera at any time. We took 10 photos for each color along with the white reference and stored the pixel RGB values. In addition, the app stores the pitch and roll angle (see Figure 1) from which every measurement was made. To make the procedure of taking the photos as similar as possible for the 24 colors, all measurements in one run were taken by one person, and images were taken with a similar distribution of angles and distances over the 24 colors. The dataset we use in subsequent analysis consist of 480 measurements taken in two runs.

During data collection, no direct measurement was available to confirm whether the lighting condition strictly corresponded to D65. We use the measured colors of the white reference to assess the deviation from this condition. The measured value along the L^* axis corresponds to 77.2% of the expected value, which can be explained by the fact that paper does not reflect all incident light. Along the b^* axis, the measured values are -3.53 ± 2.07 , whereas the D65 standard white has a value of -0.0104 , indicating a slight tendency toward blue-ish color shifts. (A larger b^* value means more blue in the color.) However, the relative error remains below 5%, and this deviation is considered negligible for our analysis. Measurements along the a^* axis remain close to the corresponding standard value.

2.2. Correction by Scaling

Our app is equipped with a simple, deterministic correction algorithm. Let (R_m, G_m, B_m) be the measured RGB values of a color card. We assume that the measured color (R_w, G_w, B_w) of the white reference is the brightest color one can measure under the ambient light. To recover the full RGB space $[0, 255]^3$ from the measurable color space $[0, R_w] \times [0, G_w] \times [0, B_w]$, we apply a channel-wise rescaling. The corrected RGB values are given by

$$\begin{pmatrix} \hat{R} \\ \hat{G} \\ \hat{B} \end{pmatrix} = \begin{pmatrix} \frac{255}{R_w} & 0 & 0 \\ 0 & \frac{255}{G_w} & 0 \\ 0 & 0 & \frac{255}{B_w} \end{pmatrix} \begin{pmatrix} R_m \\ G_m \\ B_m \end{pmatrix}.$$

2.3. Correction by Model

As a more complex approach to color correction, we fit a regression model on our measured data. To optimize the model toward reducing perceived color difference between detected and true colors, we transform the measured RGB values into the $L^*a^*b^*$ space before modeling. We consider a multi-target linear model defined by

$$\begin{pmatrix} \hat{L}^* \\ \hat{a}^* \\ \hat{b}^* \end{pmatrix} = \begin{pmatrix} a_1 \\ a_2 \\ a_3 \end{pmatrix} + \begin{pmatrix} B_{11} & B_{12} & B_{13} \\ B_{21} & B_{22} & B_{23} \\ B_{31} & B_{32} & B_{33} \end{pmatrix} \begin{pmatrix} L_m^* \\ a_m^* \\ b_m^* \end{pmatrix} + \begin{pmatrix} C_{11} & C_{12} & C_{13} \\ C_{21} & C_{22} & C_{23} \\ C_{31} & C_{32} & C_{33} \end{pmatrix} \begin{pmatrix} L_w^* \\ a_w^* \\ b_w^* \end{pmatrix} + \begin{pmatrix} D_{11} & D_{12} \\ D_{21} & D_{22} \\ D_{31} & D_{32} \end{pmatrix} \begin{pmatrix} \text{pitch} \\ \text{roll} \end{pmatrix}, \quad (1)$$

where (L_m^*, a_m^*, b_m^*) and (L_w^*, a_w^*, b_w^*) are the measured colors of a color card and the white reference, respectively, and $a_i, B_{ij}, C_{ij}, D_{ij}$ are parameters.

The model is fitted by minimizing the empirical risk associated with the loss function

$$\ell(y, \hat{y}) = \left(L^* - \hat{L}^* \right)^2 + \left(a^* - \hat{a}^* \right)^2 + \left(b^* - \hat{b}^* \right)^2,$$

where $y = (L^*, a^*, b^*)$ denotes the ground truth color and $\hat{y} = (\hat{L}^*, \hat{a}^*, \hat{b}^*)$ denotes the prediction given by the model. For simplicity, we refer to $\sqrt{\ell(y, \hat{y})}$, the Euclidean distance between y and \hat{y} , as the *Euclidean error* of a correction.

Our assumption is that the white reference can sufficiently characterize the ambient light, so that additional information of pitch and roll contributes little to color correction. We validate this assumption by comparing the full model (1) with a reduced model with $D = 0$.

3. Results

3.1. Effect of Correction

We train the full and reduced model on 80% of the measurements and test them on the remaining 20%. We apply scaling correction to the same test set. Figure 1(d) shows the empirical cumulative distribution function (ECDF) of the measurement-wise Euclidean error in the $L^*a^*b^*$ space on the test set. Although the corrected colors remain visually different from the ground truths, they reduce the gap by a large margin in comparison to raw measurements. In median, correction by scaling reduces the Euclidean error by 55% relative to uncorrected colors, while the full and reduced models yield a reduction of 65% and 66%, respectively. Without correction, only 2% of measured colors fall below the small color difference threshold (Euclidean error ≤ 6). Using correction by scaling, we increase the proportion to 26%. The full and reduced models yield a small color difference rate of 31% and 35%, respectively.

The error ECDFs of the two model variants are almost identical, which indicates that adding information about pitch and roll does not change the behavior of the model, as we expected. The statistics reported above also show no improvement of the full model over the reduced one. Thus, we focus on the reduced model in subsequent analysis.

While the error ECDF of the models lie above that of the scaling method, their confidence bands overlap. At the higher end of error distributions, we see an improvement of the models over simple scaling. The maximum error incurred by either model is lower than the scaling method.

To gain some insights into how the correction methods reduce the Euclidean error, we visualize the error per channel in Figure 2. One can observe a shift of error distribution in the L^* coordinates toward zero resulted from the correction methods, whereas the error distributions in the other two channels are all centered at approximately zero. These observations show that the correction methods are capable of

removing bias toward darker colors, but cannot eliminate uncertainty in hue.

3.2. Generalizing to Unseen Colors

Our dataset covers only 24 colors, but the models ought to generalize to arbitrary colors. We simulate the scenario of generalization to unseen colors by employing a cross-validation strategy. For each $k = 1, \dots, 20$, we randomly reserve k colors for validation and use the remaining $24 - k$ colors for training. The results are shown by Figure 3. The average-case performance of the model, measured by the average Euclidean error, remains comparable with the scaling method even if we omit up to 15 colors from the training set. When leaving out up to 5 colors, the frequency of the model achieving small color difference is, on average, higher than the scaling method, but there is large fluctuation across choices of colors to leave out.

To identify colors with high impact on generalization, we perform leave-one-out CV, training the model on all but the j -th color for $j = 1, \dots, 24$ and testing it on the single color left out. The results of leave-one-out cross validation (Figure 4) reveal an uneven distribution of generalization performance across colors. We find that color 11 is the primary driver of failure of generalization. Notably, color 11 is both a member of the Greenish group and possesses the largest green (G) channel intensity in the dataset.

Explain this color indexing.

Avoid this term.

We might need to revise the cross validation results.

4. Discussion & Conclusion

Our study provides empirical evidence that rescaling RGB channels according to a white reference can improve the quality of color measurements made by smartphones. Under usual daylight, a multi-target linear model can further avoid large deviations from the true color, although it does not prevail over the scaling method in the average case. We confirmed that the pitch and roll angle of the camera have little influence on color correction using white reference, and identified that green-toned colors play an important role in the generalization of our models.

Explain this exactly.

We acknowledge the limitations of our study and generally of color detection using smartphones. Firstly, raw camera measurements are affected by sensor noise and illumination variability. According to Gueli et al. (2019), for a better color adjustment, both black and white references should be considered. Black reference is obtained by taking a picture in a black box, such that to capture the camera noise; white reference is taken as before. The black–white correction can be implemented as an affine transformation consisting of a translation that maps the black reference to the origin of the $L^*a^*b^*$ space, and a rotation that aligns the white ref-

Table 1. Coefficient estimates on training set with 95% percentile bootstrap confidence intervals (Davison & Hinkley, 1997; Efron & Tibshirani, 1994). To construct the confidence intervals, we resample training instances with replacement, which corresponds to “resampling cases” in Davison & Hinkley (1997) and “bootstrap pairs” in Efron & Tibshirani (1994). We run 1000 bootstrap trials to obtain the confidence intervals.

	(offset)	L_m^*	a_m^*	b_m^*	L_w^*
\widehat{L}^*	80.01 [62.88, 93.33]	1.25 [1.21, 1.29]	-0.12 [-0.18, -0.11]	0.10 [0.08, 0.13]	-1.01 [-1.17, -0.77]
\widehat{a}^*	-13.91 [-34.51, -2.99]	0.02 [0.00, 0.07]	1.31 [1.29, 1.36]	-0.21 [-0.24, -0.19]	0.22 [0.07, 0.48]
\widehat{b}^*	4.94 [-12.52, 24.19]	-0.08 [-0.14, -0.05]	-0.10 [-0.13, -0.03]	1.41 [1.37, 1.44]	-0.10 [-0.34, 0.14]

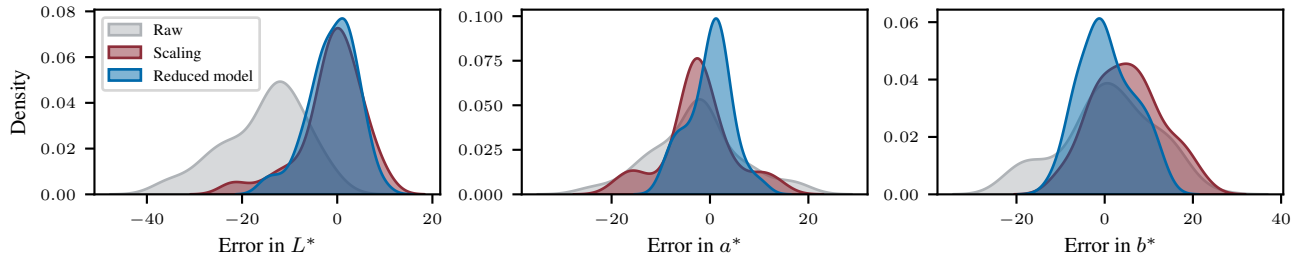


Figure 2. Kernel density plots for channel-wise difference from ground truth.

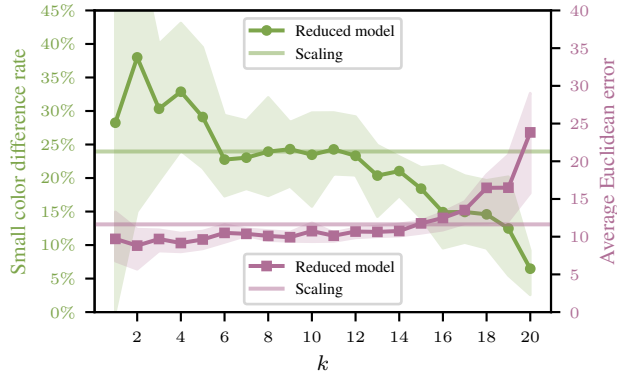


Figure 3. Validation performance of the reduced model on k left-out colors. The shaded bands show the upper and lower quartiles over 20 trials per k . The horizontal lines represent the average performance of the scaling method.

erence with the L^* axis. Secondly, given that green-toned colors appear to have high influence in the model’s generalization performance, we propose normalizing the spectral components of the light according to their relative perceptual influence. One possible implementation would be to weight each RGB coefficient by its corresponding influence prior to the conversion to $L^*a^*b^*$. After the full processing pipeline, the inverse weighting could be applied to the corrected colors in order to recover values in the original color space, while preserving the corrections introduced by the normalization and enabling a meaningful comparison with the reference.

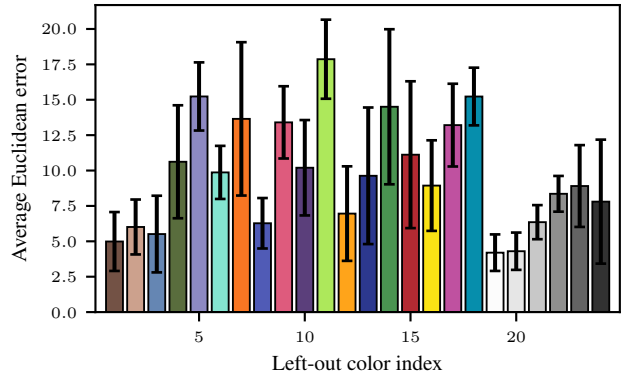


Figure 4. Validation average Euclidean error (mean \pm one standard deviation across 20 measurements) of the reduced model on single left-out color. The color of each bar is the color left out.

Contribution Statement

All authors participated in data collection. Zhi Jing performed exploratory analysis, implemented the models, and conducted preliminary experiments with them. Enrico Vesentini identified the objects that theoretically satisfy the properties required for the purposes of this study, and suggested improvements to the workflow. Tài Thái performed exploratory analysis, designed the cross validation experiments, and improved the models. Jonas Thumbs developed the app for data collection, performed exploratory analysis, and designed the graphical abstract. Baisu Zhou performed exploratory analysis, participated in implementation and analysis of the methods, and finalized the figures and the

report.

References

Davison, A. C. and Hinkley, D. V. *Bootstrap Methods and their Application*. Cambridge University Press, 1997.

Dvoretzky, A., Kiefer, J., and Wolfowitz, J. Asymptotic Minimax Character of the Sample Distribution Function and of the Classical Multinomial Estimator. *The Annals of Mathematical Statistics*, 27(3):642–669, 1956.

Efron, B. and Tibshirani, R. *An Introduction to the Bootstrap*. Chapman and Hall/CRC, 1994.

Gueli, A. M., Pasquale, S., Politi, G., and Stella, G. The role of scale adjustment in color change evaluation. *Instruments*, 3(3), 2019.

Oleari, C. *Standard Colorimetry: Definitions, Algorithms and Software*. John Wiley & Sons Inc, 2015.

Wasserman, L. *All of Statistics: A Concise Course in Statistical Inference*. Springer Texts in Statistics. Springer, 2004.